Methane-derived carbon flows into host-virus networks at different trophic levels in soil

Lee, Sungeun; Sieradzki, Ella T; Nicolas, Alexa M; Walker, Robin L; Firestone, Mary K; Hazard, Christina; Nicol, Graeme W

Published in:
Proceedings of the National Academy of Sciences of the United States of America

DOI:
10.1073/pnas.2105124118

First published: 10/08/2021

Document Version
Peer reviewed version

Methane-derived carbon flows into host-virus networks at different trophic levels in soil

Sungeun Lee[a], Ella T. Sieradzki[b], Alexa M. Nicolas[c], Robin L. Walker[d], Mary K. Firestone[b,e], Christina Hazard[a,1] and Graeme W. Nicol[a,1,2]

[a] Environmental Microbial Genomics Group, Laboratoire Ampère, École Centrale de Lyon, CNRS UMR 5005, Université de Lyon, Ecully 69134, France

[b] Department of Environmental Science, Policy and Management, University of California, Berkeley, Berkeley, CA 94720, USA

[c] Department of Plant and Microbial Biology, University of California, Berkeley, Berkeley, CA 94720, USA

[d] Scotland's Rural College, Craibstone Estate, Aberdeen, AB21 9YA, United Kingdom

[e] Earth Sciences Division, Lawrence Berkeley National Laboratory, Berkeley, CA 94720, USA

[1] CH and GWN contributed equally to this work.

[2] To whom correspondence may be addressed. Email: graeme.nicol@ec-lyon.fr

Abstract

The concentration of atmospheric methane (CH_4) continues to increase with microbial communities controlling soil-atmosphere fluxes. While there is substantial knowledge of the diversity and function of prokaryotes regulating CH_4 production and consumption, their active interactions with viruses in soil have not been identified. Metagenomic sequencing of soil microbial communities has enabled identification of linkages between viruses and hosts. However, this does not determine if these represent current or historical interactions nor whether a virus or host are active. In this study, we identified active interactions between individual host and virus populations *in situ* by following the transfer of assimilated carbon. Using DNA stable-isotope probing combined with metagenomic analyses, we characterized CH_4-fuelled microbial networks in acidic and neutral pH soils, specifically primary and secondary utilisers, together with the recent transfer of CH_4-derived carbon to viruses. Sixty-three percent of viral contigs from replicated soil incubations contained homologues of genes present in known methylotrophic bacteria. Genomic sequences of ^{13}C-

enriched viruses were represented in over one-third of spacers in clustered regularly interspaced short palindromic repeats (CRISPR) arrays of multiple, closely-related *Methylocystis* populations, and revealed differences in their history of viral interaction. Viruses infecting non-methanotrophic methylotrophs and heterotrophic predatory bacteria were also identified through the analysis of shared homologous genes, demonstrating that carbon is transferred to a diverse range of viruses associated with CH_4-fuelled microbial food networks.

Significance statement

The impact of soil viruses on prokaryotic hosts and their functional processes is largely unknown. While metagenomic sequencing of soil microbial communities enables identification of linkages between viruses and hosts, this does not necessarily identify contemporary interactions. To enable a detailed analysis of active virus-host interactions between individual populations, we focussed on the critical biogeochemical process of CH_4 oxidation and followed the transfer of carbon from hosts to their associated viruses *in situ*. Analysis of ^{13}C-enriched metagenomic DNA demonstrated that CH_4-derived carbon is transferred into viral biomass via both primary and secondary utilisers of CH_4, and suggests viral predation is an important mechanism for releasing CH_4-derived organic carbon into the soil matrix.

Introduction

Microorganisms play a central role in global carbon (C) biogeochemical cycling in soil systems. Soil is one of the most diverse habitats in the biosphere and can typically contain 10^9 -10^{10} prokaryotic cells (1) or viruses (2) per g. Infection by viruses facilitates the horizontal transfer of genes and viral lysis acts as a control of host abundance and releases nutrients. In the marine environment, 20-40% of prokaryotes are lysed on a daily basis with the release of 150 Gt of carbon annually (3). However, the role of viruses in influencing prokaryotic ecology in soil remains comparatively unknown (4). In particular, difficulties remain in identifying the frequency of active interactions between native host and virus populations *in situ*, largely due to a lack of tools to study interactions within the highly complex and heterogeneous soil environment. While red-queen or ‘arms race’ dynamics have not yet been observed in natural soil populations as they have in marine systems (5), studies have shown viruses can coevolve with their hosts in soil and that hosts

change in their susceptibility to infection (6). Shotgun sequencing of diverse soil microbial communities has enabled identification of linkages between viruses and hosts involved in carbon cycling both through identifying CRISPR protospacer sequences in viral genomes and the presence of viral genes encoding enzymes involved in complex carbon degradation (7). However, determining virus-host associations *in situ* with these methods does not typically elucidate the timeline of multiple viral infections, with linkages potentially associated with populations not active under current conditions, or even with relic DNA (8).

The atmospheric concentration of methane (CH_4) has more than doubled since the mid-eighteenth century (9), contributing 25% of additional radiative forcing from persistent greenhouse gases (10). Methanotrophs play a major role in removing atmospheric CH_4, with soils estimated to contribute 5% of the global sink (9) and mediating fluxes to the atmosphere from methanogenic activity in anoxic habitats in soil (11). Consequently, there is considerable knowledge of the diversity and functioning of CH_4-cycling microorganisms in soil (e.g. 12-17). Aerobic methanotrophs use CH_4 for both carbon and energy requirements and key representatives in soil belong to the type I Gammaproteobacteria family *Methylococcaceae*, type II Alphaproteobacteria families *Methylocystaceae* and *Beijerinckiaceae*, and *Methylacidiphilaceae* of the Verrucomicrobia (13). Soil pH is one of many factors influencing methanotroph activity and type I and type II methanotrophs can dominate activity in neutral and acidic pH soils, respectively (18). In addition, a wide variety of non-methanotrophic methylotrophs utilise methanol produced and excreted by methanotrophs, and together methanotrophic and other methylotrophic single carbon compound (C1)-utilising consortia assimilate CH_4-derived carbon in a variety of habitats (19).

Despite the substantial amount of work determining the ecophysiology of methanotrophs, very little is known about the role of viruses in influencing their ecology and functioning in any natural environment. Tyutikiv and colleagues (20, 21) characterised the morphology of *Methylosinus*-infecting viruses isolated from a range of habitats including soil, fish, bovine rumens and terrestrial water sources. More recently, metagenomic analyses have identified viruses predicted to infect methanotroph hosts in soil (7) and freshwater habitats (22), with the latter study also identifying genes encoding particulate methane monooxygenase sub-unit C (PmoC) in the genomes of giant viruses, indicating that they may have the ability to augment

the activity of infected methanotrophs. Viruses of non-methanotrophic methylotrophs have also been isolated but from non-soil environments (23-25). However, we currently have no knowledge of the dynamics of virus interactions with soil methanotroph or non-methanotrophic methylotroph populations *in situ*.

A widely used technique for identifying active populations within a diverse microbial community in environmental samples, including methanotrophs, is DNA stable isotope probing (SIP) (26). Incorporation of a substrate enriched with an isotope can be traced in genomes of community members. This can demonstrate utilisation of the original substrate thereby linking a genome to a functional process, but may also be the result of secondary utilisation i.e. incorporation of the isotope from a metabolic product or microbial biomass (27). As viruses are entirely composed of elements derived from a host cell, their production inside active hosts incorporating an isotopically-enriched substrate will also result in detectable viral isotopic enrichment (28). In this study we aimed to identify active virus-host interactions within a complex soil habitat by focussing on a taxonomically and functionally restricted group of organisms. By following ^{13}C flow *in situ*, we aimed specifically to identify DNA viruses actively infecting their methanotroph host, using CH_4-derived C, including the identification of individual virus-host interactions, and potentially those actively infecting secondary utilisers such as non-methanotrophic methylotrophs.

Results and discussion

Analysis of methane-derived ^{13}C-enriched virus and bacterial metagenomes

After aerobically incubating pH 4.5 and 7.5 soils in the presence of ^{12}C- or ^{13}C-CH_4, high buoyant density genomic DNA (>1.732 g ml^{-1}) containing ^{13}C-enriched or ^{12}C-high GC mol% genomic DNA was recovered via isopycnic centrifugation in CsCl gradients (SI Appendix, Fig. S1). Six metagenomes were produced from ^{13}C isotopically-enriched DNA samples only (three pH 4.5, three pH 7.5; SI Appendix, Table S1). Concentrations of high buoyant density genomic DNA from ^{12}C-CH_4 incubations were too low for comparable shotgun sequencing. While this indicated minimal recovery of unenriched DNA in ^{13}C-incubated samples, analysis of 16S rRNA gene amplicon libraries prepared from high buoyant density DNA of both ^{12}C and ^{13}C-CH_4 incubations confirmed ^{13}C-enrichment of C1-utilising populations (SI Appendix, Fig. S2). The most abundant families in ^{12}C amplicon libraries belonged to

the phylum Actinobacteria, containing members with high GC mol% genomes without known C1 metabolisms (i.e. *Thermomonosporaceae* and *Micrococcaceae* in pH 4.5 and 7.5 soils, respectively) whereas the most abundant families in ^{13}C amplicon libraries contained members with known C1 metabolisms (i.e. *Hyphomicrobiaceae* and *Methylococcaceae* in pH 4.5 and 7.5 soils, respectively). This indicates that high buoyant density ^{13}C-enriched metagenomic libraries represented active C1 incorporators rather than microorganisms with high GC mol% DNA.

Reads from individual metagenomes were assembled before taxonomic assignment of contigs. Reproducibly distinct communities were enriched in the two soils (SI Appendix, Fig. S2), with only six bacterial families each representing >1% of reads mapped to contigs ≥5 kb, and all including known C1-utilising taxa (*Beijerinckiaceae*, *Bradyrhizobiaceae*, *Hyphomicrobiaceae*, *Methylococcaceae*, *Methylocystaceae* and *Methylophilaceae*). We resolved twenty-three medium and high-quality (29) metagenome-assembled genomes (MAGs) (SI Appendix, Table S2), including 12 methanotrophs. Specifically, 3 MAGs represented gammaproteobacterial type I methanotrophs (*Methylobacter*) and 9 MAGs represented alphaproteobacterial type II methanotrophs (*Methylocystis*, *Methylosinus* or *Methylocapsa*). Secondary utilisers of CH_4-derived organic carbon were also identified with 9 MAGs associated with established or putative non-methanotrophic methylotrophs, lacking CH_4 oxidation machinery but capable of utilising methanotroph-derived methanol (SI Appendix). These included representatives of the *Gemmatimonadales*, *Hyphomicrobium*, *Herminiimonas* and *Rudaea*, the latter two, to our knowledge, not having been previously associated with methylotrophy but possessed predicted methanol and formate dehydrogenases (SI Appendix, Table S2). Two MAGs represented strains of *Bdellovibrio* and *Myxococcus*, known predatory bacteria (30), indicating that growing methanotrophic and methylotrophic populations were preyed upon.

Virus populations linked to C1-hosts were analysed using metagenome viral contigs (mVCs), predicted using established tools. Using contigs ≥10 kb (31), VirSorter (32) predicted 270 metagenome viral contigs (mVCs) with a further 4 ‘likely’ mVCs predicted uniquely by DeepVirFinder (33) (SI Appendix), together representing 227 viral operational taxonomic units (vOTUs) (34). Analysis of the normalised read

mapping for mVCs demonstrated that, as with the bacterial communities, active ^{13}C-enriched viral populations were reproducibly distinct between acidic and neutral pH soils (SI Appendix, Fig. S3). Analysis of free virus-targeted metagenomes (viromes) prepared from the same soil prior to CH_4 incubation (SI Appendix, Table S1) revealed that reads could be mapped to 144 (53.3%) of all ^{13}C-derived mVCs, even before enrichment for methane-utilising consortia. This indicates that the majority of mVCs identified after CH_4 incubation were from free viruses rather than those integrated in host genomes. Thirty-four percent of mVCs possessed an integrase homologue, a marker gene for a temperate life cycle, which is comparable to the proportion of temperate viruses that constitute free viruses in other environments (e.g. 35, 36). This suggests mVCs sampled in this study represent a mixture of viruses capable of lysogenic or lytic-only life cycles.

Identification of active methanotroph viruses and linkage to individual populations through analysis of CRISPR arrays

CRISPR arrays were identified in 3 of 23 MAGs, each associated with the genus *Methylocystis* or *Methylosinus* of the *Methylocystaceae* (Fig. 1). In the acidic soil, complete CRISPR arrays of growing methanotrophs were associated with two *Methylocystis* MAGs (MAG identifiers 5 and 6) sharing 79.2% average nucleotide identity (ANI) and likely representing different species (39). A further four complete and two incomplete CRISPR arrays were identified in unbinned bacterial contigs all possessing the same direct repeat (DR) sequence. These eight arrays varied in size, ranging from 9 to 114 DRs, contained a total of 432 spacers, and were in the same size range of *Methylocystaceae* CRISPR arrays from sequenced genomes (SI Appendix, Table S3). Comparison of spacer incorporation between arrays revealed that these multiple closely-related populations had different histories of viral interaction. Genome sequences from ^{13}C-enriched viral populations were represented by seven mVCs with 100% sequence identity to 29.5% of spacers. In addition, 7.9% of spacers possessed a one nucleotide mismatch, all of which represented a synonymous substitution, indicating that variation was the result of mutations in viral genomes increasing their ability to evade CRISPR-Cas defense systems or genetic variation in closely related viral populations. Only three pairs of spacers were identical, with each pair member located on a different array. Variation

in virus host range was also observed, with mVCs linked to only one or both *Methylocystis* MAGs, respectively.

Surprisingly, a large number of spacers in individual *Methylocystis* CRISPR arrays were linked to the same virus, with up to 31 being homologous to protospacer sequences in one mVC. To provide support that these multiple spacers were derived from *Methylocystis*-associated viruses, mVCs were examined for host-specific conserved protospacer-adjacent motif (PAM) sequences (40). Consistent with the identification of genuine protospacers, 138 of linked 146 spacers (i.e. all possessing ≤ 1 mismatch) had the conserved PAM sequence 'TTC' (target-centric orientation) (41). The relative position of spacers from each mVC in the arrays also revealed temporal differences in virus interaction. For example, sequences from viruses represented by mVC_12213_cat2 were present in more recently incorporated spacers in some arrays, including the latest integrated spacer in one complete array, revealing the possibility of incorporation during the incubation of the experiment.

Analysis of all CRISPR arrays (i.e. including those in unbinned contigs) revealed that the majority of linked ^{13}C-enriched viruses were associated with methanotrophic populations (Fig. 2a). In total, 11 different variants were identified (i.e. each having a unique DR sequence) with 9 linked to *Methylocystaceae* or *Methylococcaceae* populations. DR sequences generally possessed high sequence similarity to those in CRISPR arrays from genomes of cultivated strains of the same family, although only CRISPR array 6 had a DR sequence that was identical (SI Appendix, Table S3). Individual DR variants were restricted to either pH 4.5 or 7.5 soil. Using 100% sequence identity in searches between CRISPR spacer and mVC protospacer sequences, 19 VirSorter-predicted mVCs were linked to all CRISPR array variants. In addition, analysis of shorter mVCs ranging 5-10 kb identified two additional linked mVCs (mVC_08964_cat.3 (9.8 kb) and mVC_28139_DVF (5.1 kb)). One third of CRISPR linked-mVCs were categorized at the lowest level of confidence (i.e. category-3 by VirSorter (32) or 'possible' by DeepVirFinder (33), suggesting that retaining only higher confidence contigs may exclude a substantial proportion of *bona fide* methanotroph virus-derived contigs in uncharacterised environments such as soil.

Analysis of tetranucleotide frequencies (TETRA) (42) clustered the 21 mVCs into three groups that were associated with the *Methylocystaceae*, *Methylococcoceae* and an unknown group (Fig. 2b). The majority of viruses infected

members of the *Methylocystaceae* family, with those infecting populations of the *Methylocystis* and *Methylosinus* genera restricted to acidic and neutral pH soils, respectively. TETRA correlation coefficients of all *Methylocystaceae*-linked viruses were in the same range both within and between either genus, suggesting co-evolution with their host rather than genetic drift and divergence was the primary mechanism for defining specific associations with *Methylocystis* or *Methylosinus* strains.

Linkage of active viruses and hosts from analysis of shared homologues

Identification of the most abundant homologous genes between an individual mVC and one prokaryotic taxonomic family were always consistent with host-virus linkages established using spacer sequences from MAG CRISPR arrays. Specifically, BLASTp searches of genes present in the 9 mVCs linked to *Methylocystaceae* MAGs via CRISPR spacer sequences all contained 'best hits' (amino acid identity >30%, e-value $<10^{-5}$, bit score >50 and query coverage >70%) to a minimum of 5 homologues also found in *Methylocystaceae* genomes. This was therefore used as a further criterion for establishing host-virus linkages. Analysis of assembled contigs from twelve metagenomic libraries of total community or virome DNA from the same soil samples without CH_4 incubation (SI Appendix, Table S1) contained only three VirSorter-predicted mVCs that were linked to methanotrophs. In contrast, using a ^{13}C-targeted approach, 63% of mVCs contained a homologue that was linked to genomes of known C1-utilising bacteria, with 35% linked specifically to populations from the *Methylocystaceae*, *Methylococcaceae* or *Hyphomicrobiaceae* (Fig. 3a). While analysis of bacterial homologues in mVCs identified the taxonomic family of the assumed dominant host, they also indicated that individual viruses may infect hosts of other families of the same taxonomic order, including those at other trophic levels. Specifically, within the *Rhizobiales*, mVCs linked to *Methylocystaceae* also contained homologues shared with *Bradyrhizobiaceae*, *Methylobacteriaceae* and *Rhizobiaceae* (Fig. 3b), indicating that viruses of methanotrophs may also infect non-methanotrophic methylotrophs that are active at the same time.

Methane-derived carbon in viruses of hosts from different trophic levels

CH_4-derived C was also transferred to viruses of secondary (and potentially tertiary) utilisers. One group of mVCs were linked to methylotrophic *Hyphomicrobiaceae* and

a second to a phylogenetically diverse range of nitrogen-fixing Rhizobia i.e. *Bradyrhizobiaceae*, *Phyllobacteriaceae* and *Rhizobiaceae*. These lineages contain known methylotrophs, methanol dehydrogenases have been identified in a range of rhizobial species (43) and these mVCs also contained homologues found in the genomes of nodulating *Methylobacterium* strains (44). Viruses of predatory *Bdellovibrio* and *Myxococcales* bacteria were predicted, consistent with the recovery of corresponding bacterial MAGs in ^{13}C-enriched DNA. One mVC (20210-cat_2) was linked to the genus *Bdellovibrio* and three were linked to *Myxococcales* populations, containing gene homologous to four families within the order. While the latter were category-3 mVCs (i.e. possible viruses), *Myxococcales*-associated contigs were also predicted as viral in origin using other tools (45, 46). The high isotopic labelling of both heterotrophic predators (with no identifiable C1-utilising capability) and their viruses indicate that the predators were feeding primarily on populations that incorporated CH_4-derived carbon i.e. methanotrophs, non-methanotrophic methylotrophs or other organisms consuming metabolic products or biomass, as feeding on unlabelled bacteria would dilute their enrichment. While the path of carbon flow to predatory bacteria is uncertain, it indicates that they have a preference for preying upon growing populations rather than the majority not incorporating CH_4-derived C (27).

Gene-sharing network analysis of mVCs with viruses in the NCBI RefSeq database and other metagenome studies were analysed using vConTACT 2.0 (47). Any linkages with RefSeq viruses typically had low scores (i.e. sharing a low number of homologues) and were linked to viruses of hosts that were inconsistent with our homologue-based predictions (SI Appendix, Table S4). No linkages were observed with recently reported giant viruses of methanotrophs in freshwater lakes (22). However, in a recent study of 197 metagenomes from Swedish peatland soil, Emerson *et al.* (7) identified 13 viruses linked to methanotrophs. Intriguingly, 8 of these were linked in our viral gene-sharing network, with both studies predicting *Methylocystaceae* hosts using different approaches for linkage prediction (SI Appendix, Fig. S4) and revealing the distribution of specific *Methylocystaceae*-associated viral groups present in different geographical areas and soil types. Analysis of gene-sharing networks of mVCs from this study indicated that there were two distinct *Methylocystaceae*-linked viral clusters which also varied in their distribution in both soils. Specifically, one cluster was associated with low pH only

whereas the second cluster contained viruses found in both pH 4.5 and 7.5 soils, including those linked by CRISPR spacer sequences. Individual networks of *Methylococcaceae*- and rhizobia-associated mVCs were also identified, associated with one of the two soils of contrasting pH. Taxonomically-linked mVCs with ≥5 homologues were consistently placed in networks with other mVCs containing 1-4 homologues from the same methylotrophic families, confirming host linkage to a larger number of mVCs.

Genomic content of ^{13}C-enriched viral contigs

mVCs contained 8,174 genes, with 49.6% (4,054) annotated and representing 606 unique functions. Of these, genes encoding viral proteins accounted for 9.8% (397 genes) and included major capsid proteins, tail proteins, integrases, portal proteins and terminases. Bacterial proteins used for viral replication accounted for 5.1% (206 genes). A number of metagenomic studies have demonstrated that viruses can possess genes encoding sub-unit C of ammonia or particulate methane monooxygenases as auxiliary metabolic genes (AMGs) (48,22) which are also typically found as isolated genes in genomes in addition to being present in clusters or operons encoding A and B sub-units (49). In this study, one low confidence mVC (7.3 kb, category-3) was identified as containing an isolated *pmoC* gene that was phylogenetically related to growing *Methylocystis* populations but was distinct from *pmoC* sequences found in viruses associated with freshwater *Methylocystis* populations[33] (SI Appendix, Fig. S5).

Conclusions

These results demonstrate that by following carbon flow, native virus-host interactions associated with a critical biogeochemical process can be identified at the resolution of individual populations. Active interactions were observed at different trophic levels within the highly complex soil environment, from primary utilisers of CH_4 to heterotrophic bacteria preying upon ^{13}C-enriched methylotrophs or other organisms consuming CH_4-derived metabolic products or biomass. Therefore, viral lysis may be an important mechanism for the transfer of CH_4-derived organic carbon into a soil viral shunt. Type I and II methanotrophs interact with distinct groups of viruses and the composition of CRISPR arrays of *Methylocystaceae* reveal that they

have a continual dynamic interaction with specific viral populations. Analysis of shared homologues in individual viral genomes show that they may also interact with host populations at different trophic levels within a CH_4-fuelled network.

Methods

Soil microcosms

Triplicate soil samples were collected in February 2018 at 1 m intervals from the upper 10 cm of pH 4.5 and 7.5 soil sub-plots of a pH gradient maintained since 1961 and under an 8-year crop rotation (SRUC, Craibstone Estate, Aberdeen, Scotland; UK grid reference NJ872104) (50). The crop at the time of sampling was potatoes. Soil (podzol, sandy-loam texture) was sieved (2 mm mesh size) and microcosms established in triplicate for each soil pH and isotope in 144 ml serum bottles containing 14.30 g soil (10 g dry weight equivalent) with a 30% volumetric water content, equivalent to ~60% water-filled pore space. Bottles were capped and established with a 10% (v/v) ^{12}C-CH_4 or ^{13}C-CH_4 (Sigma-Aldrich) headspace (99% atom enriched), re-opening every 10 days to maintain aerobic conditions before sealing and re-establishing CH_4 headspace concentrations. Microcosms were incubated at 25^{o}C and destructively sampled after 30 days with soil archived immediately at -20^{o}C.

DNA extraction and stable-isotope probing

Genomic DNA was extracted from 0.5 g soil samples using a CTAB buffer phenol:chloroform: isoamyl alcohol bead-beating protocol and subjected to isopycnic centrifugation in CsCl gradients, recovery and purification as previously described (51). Briefly, 6 ug of genomic DNA was added to 8 ml CsCl-Tris EDTA solution (refractive index (RI) of 1.4010; buoyant density of 1.71 g ml^{-1}) in polyallomer tubes before sealing and ultracentrifugation at 152,000 × *g* (50,000 rpm) in a MLN80 rotor (Beckman-Coulter) for 72 h at 25°C. CsCl gradients were fractionated into 350 ul aliquots using an in-house semi-automated fraction recovery system before determining RI and recovering DNA. The relative abundance of bacterial 16S rRNA and methanotrophic *pmoA* genes in genomic DNA distributed across the CsCl gradients was determined by qPCR in a Corbett Rotor-Gene 6000 thermocycler (Qiagen) using primer sets P1(341f)/P2(534r) (52) and A189F/A682R (53) respectively. Twenty-five µl reactions contained 12.5 µl 2X QuantiFast SYBR Green

Mix (Qiagen), 1 µM of each primer, 100 ng of T4 gene protein 32 (Thermo Fisher), 2 µl of standard (10^8-10^2 copies of an amplicon-derived standard) or 1/10 diluted DNA. Thermocycling conditions consisted of an initial denaturation step of 15 min at 95°C for both assays followed by 30 cycles of 15 s at 94°C, 30 s at 60°C, 30 s at 72°C for the 16S rRNA gene assay or 60 s at 94°C, 60 s at 56°C, 60 s at 72°C for the *pmoA* gene assay, followed by melt-curve analysis. All assays had an efficiency between 93-97% with an r^2 value >0.99. Genomic DNA from four fractions with a buoyant density >1.732 g ml^{-1} were then pooled for each ^{12}C- and ^{13}C-CH_4-incubated replicate for 16S rRNA gene amplicon sequence and metagenomic analysis.

DNA extraction for soil virome analysis is summarised in the SI Appendix.

Metagenome sequencing, assembly and annotation

Library preparation and sequencing was performed at the Joint genome Institute (JGI), Berkeley, USA. Libraries were produced from fragmented DNA using KAPA Biosystems Library Preparation Kits (Roche) and quantified using KAPA Biosystems NGS library qPCR kits. Indexed samples were sequenced (2 x 150 bp) on the Illumina NovaSeq platform with NovaSeq XP v1 reagent kits and a S4 flowcell. Raw reads were processed with JGI's RQCFilter2 pipeline that utilised BBTools v38.51 (54). Reads containing adapter sequences were trimmed and those with ≥3 N bases or ≤51 bp or ≤33% of full-read length were removed along with PhiX sequences using BBDuk, and reads mapped to human, cat, dog or mouse references at 95% identity were removed using BBMap. *De novo* contig assembly of the 100 - 196 million quality-controlled reads per metagenome was performed using MetaSPAdes v3.13.0 (55). The 1 - 2 million contigs per metagenome were then concatenated together, and contigs larger than 5 kb were dereplicated at 99% average nucleotide identity (ANI) using PSI-CD-HIT v4.6.1 (56) and binned using MetaWRAP v1.2.1 (57) (SI Appendix, Table S5). Bin completion and contamination was determined by CheckM v1.0.12 (58). Taxonomic annotation of contigs was performed using Kaiju (59) with the NCBI RefSeq database (Release 94; 25 June 2019) (60) and MAGs using GTDB-Tk v0.3.2 (61) with the Genome Taxonomy Database (release 89, 21 June 2019) (62). Protein sequence annotation was performed using InterProScan 5 (e-value $<10^{-5}$) (63). Pairwise ANI comparison of MAGs was calculated using FastANI (39).

406 *Amplicon sequencing and analysis*

407 16S rRNA genes were amplified using primers 515F/806R (64) followed by library
408 preparation and sequencing on an Illumina MiSeq sequencer as previously
409 described (65). Reads with a quality score <20 and length < 100 bp were discarded
410 using FASTX-Toolkit v0.0.13 (http://hannonlab.cshl.edu/fastx_toolkit/). High-quality
411 reads were merged using PANDAseq v2.11 (66), and denoising and chimera
412 removal performed with UNOISE3 (67). Amplicon sequence variants (ASVs) were
413 annotated using the RDP classifier v2.11 (68). Non-metric multidimensional scaling
414 of Bray-Curtis dissimilarity derived from the relative abundance of ASVs was
415 performed with the metaMDS function in the vegan package (69) in R v3.6.0.

416

417 *Virus prediction*

418 Metagenomic viral contigs (mVCs) were predicted from 9,190 contigs >10 kb using
419 VirSorter (32), retaining non-prophage category-1, -2 or -3 mVCs, representing “most
420 confident”, “likely” and “possible”. DeepVirFinder (33) was also used to predict mVCs
421 from contigs >10 kb, with those with a *p*-value <0.05 and a score ≥0.9 or ≥0.7,
422 representing “confident” and “possible”, respectively (SI Appendix, Table S6). The
423 relative abundance of each mVC in the six metagenomes was determined using the
424 MetaWRAP-Quant_bins module (57) and a heatmap produced using the heatmaply
425 package in R v3.6.0. The tools CheckV (45) and VIBRANT (46) were also used to
426 predict a viral origin of category-3 *Myxococcales*-associated mVCs.

427

428 *Virus-host linkage*

429 CRISPR arrays within MAGs and unbinned contigs were identified using the
430 CRISPR Recognition Tool (CRT) v1.2 (37) (SI Appendix, Table S7). DR and spacer
431 sequences were extracted before performing 100% identity searches against
432 positive and negative strands to identify MAGs or contigs with direct repeats and the
433 viral origin of spacers using Seqkit commands (38). After identification of matched
434 spacer sequences in mVCs, 10 nucleotides before and after the spacer sequence
435 were extracted to identify associated host-specific PAM sequences. Conserved and
436 variant PAM sequences were manually identified. Correlation coefficients of pairwise
437 comparison of the tetra-nucleotide frequencies between unique CRISPR-associated
438 mVCs were calculated using Python package pyani v0.2.10 (70). To identify
439 homologous genes shared between CRISPR-linked viruses and hosts, gene

prediction was performed using Prodigal v2.6.3 (71) with the -p meta option followed by protein alignment with Blastp (identity >30%, e-value < 10^{-5}, bit score >50 and query cover >70%) and protein sequence annotation using InterProScan 5 (e-value <10^{-5}). Gene homology between all mVCs and prokaryotes in the NCBI nr database was determined using Diamond Blastp (e-value <10^{-5}) (72). Virus-host prediction using *k*-mer frequencies was performed with WIsH v1.0 (73). Networks based on shared gene content was constructed using vConTACT 2.0 (47) with the NCBI RefSeq database (Release 94; 25 June 2019).

Phylogenetic analysis of PmoC and PxmC protein sequences

Maximum likelihood analysis of inferred protein sequences of membrane-bound monooxygenase C sub-units from methanotroph MAGs and reference sequences (SI Appendix, Table S8) was performed on 229 unambiguously aligned sequences using PhyML 3.0 (74) with automatic model selection (LG substitution, gamma distribution (0.06) and proportion of invariable sites (0.087) estimated). Bootstrap support was calculated from 100 replicates.

Data availability

Metagenome sequence reads are deposited under NCBI BioProject accession numbers PRJNA621430 - PRJNA621435. Metagenome draft assemblies are accessible through the JGI Genome Portal (DOI: 10.25585/1487501). Amplicon sequence data is deposited in the NCBI Sequence Read Archive with BioProject accession number PRJNA676099.

Acknowledgments

This work was funded by an AXA Research Chair awarded to GWN, a France-Berkeley Fund grant (2018-2019) awarded to GWN and MKF, and the U.S. Department of Energy Office of Science, Office of Biological and Environmental Research Genomic Science Program under award DE-SC0010570 to MKF. The sequencing data were generated under JGI Community Science Program proposal 503702 awarded to GWN and CH. The work conducted by the U.S. Department of Energy Joint Genome Institute, a DOE Office of Science User Facility, is supported by the Office of Science of the U.S. Department of Energy under Contract No. DE-AC02-05CH11231. The pH gradient experiment is funded through the Scottish

Government RESAS 2016-2021 programme. The authors would like to thank Prof. Joanne Emerson for valuable discussion, and Dr. Laurent Pouilloux for assistance with the Newton high performance computing cluster at École Centrale de Lyon.

Author contributions

The research programme was conceived by and funded from grants awarded to GWN, CH and MKF. SL, CH and GWN designed the experiment and wrote the manuscript. SL performed experiments and analyses. ES, AN and MKF advised on bioinformatic approaches, discussed data and commented on the manuscript. RW coordinated soil sampling and commented on the manuscript. All authors approved the manuscript.

References

1. Frossard, A., Hammes, F., Gessner, M.O. Flow cytometric assessment of bacterial abundance in soils, sediments and sludge. *Front. Microbiol.* **7**, 903 (2016).
2. Williamson, K.E., Fuhrmann, J.J., Wommack, K.E., Radosevich, M. Viruses in soil ecosystems: an unknown quantity within an unexplored territory. *Annu. Rev. Virol.* **4**, 201-219 (2017).
3. Suttle, C. A. Marine viruses—major players in the global ecosystem. *Nat. Rev. Microbiol.* **5**, 801–812 (2007).
4. Emerson, J.B. Soil viruses: A new hope. *mSystems* **4**, e00120-19 (2019).
5. Ignacio-Espinoza, J. C., Ahlgren, N.A., Fuhrman, J.A. Long-term stability and Red Queen-like strain dynamics in marine viruses. *Nat. Microbiol*. 5, 265-271 (2020).
6. Gómez, P., Buckling. Bacteria-phage antagonistic coevolution in soil. *Science* **332**, 106-109 (2011).
7. Emerson, J.B. *et al*. Host-linked soil viral ecology along a permafrost thaw gradient. *Nat. Microbiol*. **3**, 870-880 (2018).
8. Carini, P., Marsden, P.J., Leff, J.W., Morgan, E.E., Strickland, M.S., Fierer N. Relic DNA is abundant in soil and obscures estimates of soil microbial diversity. *Nat. Microbiol.* **2**, 16242 (2017).
9. Saunois, M. *et al.* The Global Methane Budget 2000–2017. *Earth Syst. Sci. Data* **12,** 1561–1623 (2020).

10. Etminan, M., Myhre, G., Highwood, E.J., Shine, K.P. Radiative forcing of carbon dioxide, methane, and nitrous oxide: A significant revision of the methane radiative forcing. *Geophys. Res. Lett.* 12, 614-623 (2016).
11. Le Mer, J., Roger, P. Production, oxidation, emission and consumption of methane by soils: a review. *Eur. J. Soil Biol.* **37**, 25–50 (2001).
12. Angel, R., Claus, P., Conrad, R. Methanogenic archaea are globally ubiquitous in aerated soils and become active under wet anoxic conditions. *ISME J.* **6**, 847-862 (2012).
13. Knief, C. Diversity and habitat preferences of cultivated and uncultivated aerobic methanotrophic bacteria evaluated based on pmoA as molecular marker. *Front. Microb*. **6**, 1346 (2015).
14. Lyu, Z., Shao, N., Akinyemi, T., Whitman, W.B. Methanogenesis. *Curr. Biol.* **28**, 727–732 (2018).
15. Morris, S.A., Radajewski, S. Willison, T.W., Murrell, J.C. Identification of the functionally active methanotroph population in a peat soil microcosm by stable-isotope probing. *Appl. Environ. Microbiol.* **68**, 1446-1453 (2002).
16. Pratscher, J., Vollmers, J., Wiegand, S., Dumont, M.G., Kaster, A.-K. Unravelling the identity, metabolic potential and global biogeography of the atmospheric methane-oxidizing Upland Soil Cluster α. *Environ. Microbiol*. **20**, 1016-1029 (2018).
17. Tveit, A.T., *et al.* Widespread soil bacterium that oxidizes atmospheric methane. *Proc. Natl. Acad. Sci. U.S.A.* **116**, 8515-8524
18. Zhao, J., Cai, Y., Jia, Z. The pH-based ecological coherence of active canonical methanotrophs in paddy soils. *Biogeosciences* **17**, 1451–1462 (2020).
19. Chistoserdova, L., Kalyuzhnaya, M.G., Lidstrom, M.E. The expanding world of methylotrophic metabolism. *Annu. Rev. Microbiol.* **63**, 477–499 (2009).
20. Tyutikov, F.M., Bespalova, I.A., Rebentish, B.A., Aleksandrushkina, N.N., Krivisky, A.S. Bacteriophages of methanotrophic bacteria. *J. Bacteriol.* **144**, 375-381 (1980).
21. Tyutikov, F.M., *et al.* Bacteriophages of methanotrophs isolated from fish. *Appl. Environ. Microbiol.* **46**, 917-924 (1983).
22. Chen, L.-X. *et al*. Large freshwater phages with the potential to augment aerobic methane oxidation. *Nat. Microbiol.* **5**, 1504-1515 (2020).

23. Almumin, S., Kadri, M., Mamat, U., Engel, J. Isolation and primary characterization of a new bacteriophage of obligate methylotrophic bacteria. *J. Basic Microbiol.* 30, 627-633 (1990).
24. Buchholz, H.H. *et al.* Efficient dilution-to-extinction isolation of novel virus–host model systems for fastidious heterotrophic bacteria. *ISME J.* 10.1038/s41396-020-00872-z (2021).
25. Yang, M. *et al.* Genomic Characterization and Distribution Pattern of a Novel Marine OM43 Phage. *Front. Microbiol.* **12**, 651326 (2021).
26. Radajewski, S., *et al*. Identification of active methylotroph populations in an acidic forest soil by stable-isotope probing. *Microbiol*. **148**, 2331–2342 (2002).
27. Hungate, B. *et al.* The Functional Significance of Bacterial Predators. *mBio* **12**, e00466-21 (2021).
28. Pasulka, A.L. *et al*. Interrogating marine virus-host interactions and elemental transfer with BONCAT and nanoSIMS-based methods. *Environ. Microbiol*. **20**, 671-692 (2018).
29. Bowers, R.M. *et al*. Minimum information about a single amplified genome (MISAG) and a metagenome-assembled genome (MIMAG) of bacteria and archaea. *Nat. Biotech.* **35**, 725-731 (2017).
30. Pérez, J. Moraleda-Muñoz, A., Marcos-Torres, F.J., Muñoz-Dorado, J. Bacterial predation: 75 years and counting! *Environ. Microbiol.* **18**, 766–779 (2018).
31. Roux, S. *et al*. Minimum information about an uncultivated virus genome (MIUViG). *Nat. Biotechnol.* **37**, 29–37 (2019).
32. Roux, S., Enault, F., Hurwitz, B. L., Sullivan, M. B. VirSorter: mining viral signal from microbial genomic data. *PeerJ* **3**, e985 (2015).
33. Ren, J. *et al*. Identifying viruses from metagenomic data by deep learning. *Quant. Biol.* **8,** 64-77 (2020).
34. Paez-Espino, D., Pavlopoulos, G.A., Ivanova, N.N., Kyrpides, N.C. Nontargeted virus sequence discovery pipeline and virus clustering for metagenomic data. *Nat. Protoc*. **12**, 1673 (2017).
35. Sausset, R., Petit, M.A., Gaboriau-Routhiau, V. De Paepe, M. New insights into intestinal phages. *Mucosal. Immunol.* **13,** 205–215 (2020).
36. Jahn, M.T. *et al.* Lifestyle of sponge symbiont phages by host prediction and correlative microscopy. *ISME* J. 10.1038/s41396-021-00900-6 (2021).

37. Bland, C. *et al*. CRISPR Recognition Tool (CRT): a tool for automatic detection of clustered regularly interspaced palindromic repeats. *BMC Bioinform*. **8**, 209 (2007).
38. Shen, W., Le, S., Li, Y., Hu, F. SeqKit: A cross-platform and ultrafast toolkit for FASTA/Q file manipulation. *PLoS ONE* **11**, e0163962 (2016).
39. Jain, C., Rodriguez-R, L.M., Phillippy, A.M., Konstantinidis, K.T. High throughput ANI analysis of 90K prokaryotic genomes reveals clear species boundaries. *Nature Comm.* **9**, 5114 (2018).
40. Mojica, F.J.M., Díez-Villaseñor, C., García-Martínez, J., Almendros, C. Short motif sequences determine the targets of the prokaryotic CRISPR defence system. *Microb.* **155**, 733-740 (2009).
41. Leenay, R.T., Beisel, C.L. Deciphering, communicating, and engineering the CRISPR PAM. J. Mol. Biol. **429,** 177-191 (2017).
42. Wang, J. *et al*. Genomic sequence of *'Candidatus* Liberibacter solanacearum' haplotype C and its comparison with haplotype A and B genomes. *PLoS One* **12,** e0171531 (2017).
43. Huang, J. *et al*. Rare earth element alcohol dehydrogenases widely occur among globally distributed, numerically abundant and environmentally important microbes. *ISME J.* **13**, 2005-2017 (2019).
44. Green, P.N, Ardley, J.K. Review of the genus *Methylobacterium* and closely related organisms: a proposal that some *Methylobacterium* species be reclassified into a new genus, *Methylorubrum* gen. nov. *Int. J. Syst. Evol. Microbiol.* **68**, 2727-2748 (2018).
45. Stephen Nayfach *et al.* CheckV assesses the quality and completeness of metagenome-assembled viral genomes. *Nat. Biotechnol.* **39**, 578–585 (2021).
46. Kieft, K., Zhou, Z., Anantharaman, K. VIBRANT: automated recovery, annotation and curation of microbial viruses, and evaluation of viral community function from genomic sequences. *Microbiome* **8**, 90 (2020).
47. Jang, H.B. *et al*. Taxonomic assignment of uncultivated prokaryotic virus genomes is enabled by gene-sharing networks. *Nat. Biotechnol*. **37**, 632-639 (2019).
48. Ahlgren, N.A., Fuchsman, C.A., Rocap, G., Fuhrman, J.A. Discovery of several novel, widespread, and ecologically distinct marine Thaumarchaeota viruses that encode *amoC* nitrification genes. *ISME J.* 13, 618-631 (2019).

49. Nicol, G.W., Schleper C. Ammonia-oxidising Crenarchaeota: important players in the nitrogen cycle? *Trends Microbiol*. **14**, 207–212 (2006).
50. Kemp, J.S., Paterson, E., Gammack, S.M., Cresser, M.S., Killham, K. Leaching of genetically modified *Pseudomonas fluorescens* through organic soils: influence of temperature, soil pH, and roots. *Biol. Fert. Soils* **13**, 218–224 (1992).
51. Nicol, G.W., Prosser, J.I. Strategies to determine diversity, growth and activity of ammonia oxidising archaea in soil. *Meth. Enzymol*. **496**, 3-34 (2011).
52. Muyzer, G., De Waal, E.C., Uitterlinden, A.G. Profiling of complex microbial populations by denaturing gradient gel electrophoresis analysis of polymerase chain reaction-amplified genes coding for 16S rRNA. *Appl. Environ. Microbiol*. **59**, 695-700 (1993).
53. Holmes, A.J., Costello, A., Lidstrom, M.E., Murrell, J.C. Evidence that particulate methane monooxygenase and ammonia monooxygenase may be evolutionarily related. *FEMS Microbiol. Lett.* **132**, 203-208 (1995).
54. Bushnell, B. BBTools software package. http://sourceforge net/projects/bbmap (2016).
55. Nurk, S., Meleshko, D., Korobeynikov, A., Pevzner, P.A. metaSPAdes: a new versatile metagenomic assembler. *Genome Res*. **27**, 824-834 (2017).
56. Fu, L., Niu, B., Zhu, Z., Wu, S., Li, W. CD-HIT: accelerated for clustering the next-generation sequencing data. *Bioinformatics* **28**, 3150-3152 (2012).
57. Uritskiy, G.V., DiRuggiero, J., Taylor, J. MetaWRAP- a flexible pipeline for genome-resolved metagenomic data analysis. *Microbiome* **15**, 158 (2018).
58. Parks, D. H., Imelfort, M., Skennerton, C. T., Hugenholtz, P., Tyson, G. W. CheckM: assessing the quality of microbial genomes recovered from isolates, single cells, and metagenomes. *Genome Res.* **25**, 1043–1055 (2015).
59. Menzel, P., Ng, K.L., Krogh, A. Fast and sensitive taxonomic classification for metagenomics with Kaiju. *Nat. Comm*. **7**, 11257 (2016).
60. O'Leary, N.A. *et al*. Reference sequence (RefSeq) database at NCBI: current status, taxonomic expansion, and functional annotation. *Nucleic Acids Res*. **44**, D733-D745 (2016).
61. Chaumeil, P-A., Mussig, A.J., Hugenholtz, P., Parks, D.H. GTDB-Tk: a toolkit to classify genomes with the Genome Taxonomy Database. *Bioinformatics* **36**, 1925-1927 (2019).

62. Parks, D.H. *et al*. A standardized bacterial taxonomy based on genome phylogeny substantially revises the tree of life. *Nat. Biotechnol*. **36**, 996-1004 (2018).
63. Jones, P. *et al*. InterProScan 5: genome-scale protein function classification. *Bioinformatics* **30**, 1236-1240 (2015).
64. Walters, W. *et al*. Improved bacterial 16S rRNA gene (V4 and V4-5) and fungal internal transcribed spacer marker gene primers for microbial community surveys**.** *mSystems* **1**, e00009-15 (2015).
65. Finn, D.R., Lee, S., Lazén, M.B., Nicol, G.W., Hazard, C. Cropping systems that improve richness convey greater resistance and resilience to soil fungal, relative to prokaryote, communities. Preprint at https://doi.org/10.1101/2020.03.15.992560 (2020).
66. Masella, A.P., Bartram, A.k., Truszkowski, J.M., Brown, D.G., Neufeld, J.D. PANDAseq: paired-end assembler for illumina sequences. *BMC Bioinform.* **13**, 31 (2012).
67. Edgar, R.C. UNOISE2: improved error-correction for Illumina 16S and ITS amplicon sequencing. Preprint at https://doi.org/10.1101/081257 (2016).
68. Wang, Q., Garrity, G.M., Tiedje, J.M., Cole, J.R. Naïve bayesian classifier for rapid assignment of rRNA sequences into the new bacterial taxonomy. *Appl. Environ. Microbiol*. **73**, 5261-5267 (2007).
69. Oksanen, J. *et al*. vegan: Community Ecology Package. https://CRAN.R-project.org/package=vegan (2019).
70. Pritchard, L., Glover, R.H., Humphris, S., Elphinstone, J.G., Toth, I.K. Genomics and taxonomy in diagnostics for food security: soft-rotting enterobacterial plant pathogens. Anal. Methods **8**, 12-24 (2016).
71. Hyatt, D. *et al*. Prodigal: prokaryotic gene recognition and translation initiation site identification. *BMC Bioinform*. **11**, 119 (2010).
72. Buchfink, B., Xie, C., Huson, D.H. Fast and sensitive protein alignment using DIAMOND. *Nat. Methods* **12**, 59-60 (2015).
73. Galiez, C, Siebert, M., Enault, F., Vincent, J., Söding, J. WisH: who is the host? Predicting prokaryotic hosts from metagenomic phage contigs. *Bioinformatics* **33**, 3113-3114 (2017).

74. Guindon, S. *et al*. New algorithms and methods to estimate maximum-likelihood phylogenies: Assessing the Performance of PhyML 3.0. *Syst. Biol*. **59**, 307-21 (2010).

677 **Figure legends**

678 **Fig. 1.** Active ^{13}C-enriched viruses of individual *Methylocystaceae* populations
679 identified from spacer sequences in CRISPR arrays. (A) and (B) Schematic
680 representation of linkages between individual mVCs and *Methylocystis* or
681 *Methylosinus* MAGs, respectively. Shared host spacer/virus protospacer sequences
682 were identified with complete identity or 1 mismatch. Numbers in hexagons denote
683 mVC IDs, with an unconnected hexagon linked to unbinned CRISPR arrays only. (C)
684 and (D) Distribution of spacers from 7 mVCs in *Methylocystis* CRISPR arrays (MAGs
685 5, 6 and six unbinned contigs), and 2 mVC in *Methylosinus* MAG 11's CRISPR array,
686 respectively. CRISPR array names describe the individual soil microcosm from
687 which a contig was derived. DRs for complete arrays are numbered (in grey), with
688 the spacer after DR 1 being the most recently incorporated. Two partial arrays are
689 denoted with an *. Spacers with complete identity or 1 mismatch to sequences in
690 mVCs are represented by colour-coded squares and circles, respectively, with
691 stripes highlighting sequences found in two different mVCs. Spacer sequences were
692 identified and matched to mVCs using the tools CRT (37) and Seqkit (38),
693 respectively.
694
695 **Fig. 2.** Linkages of ^{13}C-enriched viruses to CRISPR arrays in pH 4.5 and 7.5 soil.
696 (A) Presence of spacers from 21 mVCs (hexagon symbols) in 11 different CRISPR
697 array variants (unique DR sequence). Taxonomic affiliation of CRISPR arrays to host
698 families was determined by phylogenomic analysis of affiliated MAGs (3, 6) or
699 unbinned contigs (4, 5, 7-9), or inferred from shared homologues between linked
700 mVCs and bacterial genomes (10, 11). mVC names also describe prediction by
701 VirSorter (cat.2 or cat.3) or by DeepVirFinder alone (DVF). All mVCs were >10 kb
702 except mVC_08964_cat.3 (9.8 kb) and mVC_28139_DVF (5.1 kb). These mVCs
703 were also the only two predicted using DeepVirFinder, with calculated probabilities
704 describing 'likely' and 'probable' viruses, respectively. (B) TETRA correlation
705 coefficients between 21 CRISPR-linked mVCs. Colour-coded hexagon symbols
706 denote mVCs linked to CRISPR arrays in Fig. 1.
707
708 **Fig. 3.** Linkage of ^{13}C-enriched viruses to methanotrophic, methylotrophic
709 and predator bacterial host populations through identification of
710 shared homologous genes. (A) Association of viruses with different bacterial families

711 and functional groups inferred from the presence of ≥5 shared homologous genes,
712 with number of category-1, -2 and -3 VirSorter-predicted mVCs given. (B) Proportion
713 of homologues in methanotroph, non-methanotrophic methylotroph or predator
714 viruses linked to individual bacterial families. Each chart summarises those mVCs
715 that all contain ≥5 homologues to one family (number of mVCs given in parentheses)
716 but with other taxonomic linkages also given. ‘Other’ describes the proportion found
717 in families each represented by less than <5% of homologues or those not annotated
718 to the family level.

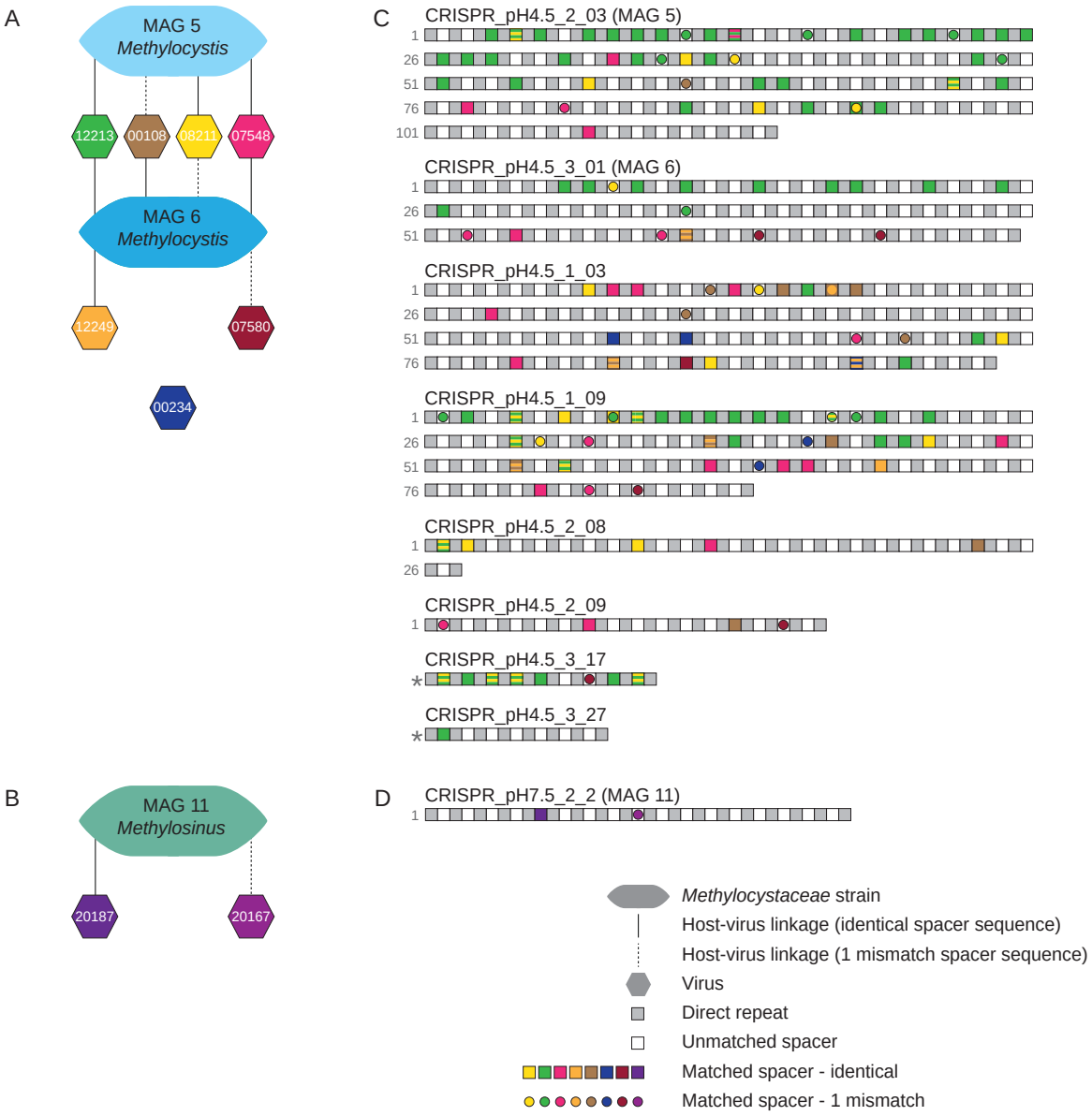
A
MAG 5
Methylocystis
12213
00108
08211
07548
MAG 6
Methylocystis
12249
07580
00234
B
MAG 11
Methylosinus
20187
20167
C
CRISPR_pH4.5_2_03 (MAG 5)
1
26
51
76
101
CRISPR_pH4.5_3_01 (MAG 6)
1
26
51
CRISPR_pH4.5_1_03
1
26
51
76
CRISPR_pH4.5_1_09
1
26
51
76
CRISPR_pH4.5_2_08
1
26
CRISPR_pH4.5_2_09
1
CRISPR_pH4.5_3_17
*
CRISPR_pH4.5_3_27
*
D
CRISPR_pH7.5_2_2 (MAG 11)
1
Methylocystaceae strain
Host-virus linkage (identical spacer sequence)
Host-virus linkage (1 mismatch spacer sequence)
Virus
Direct repeat
Unmatched spacer
Matched spacer - identical
Matched spacer - 1 mismatch

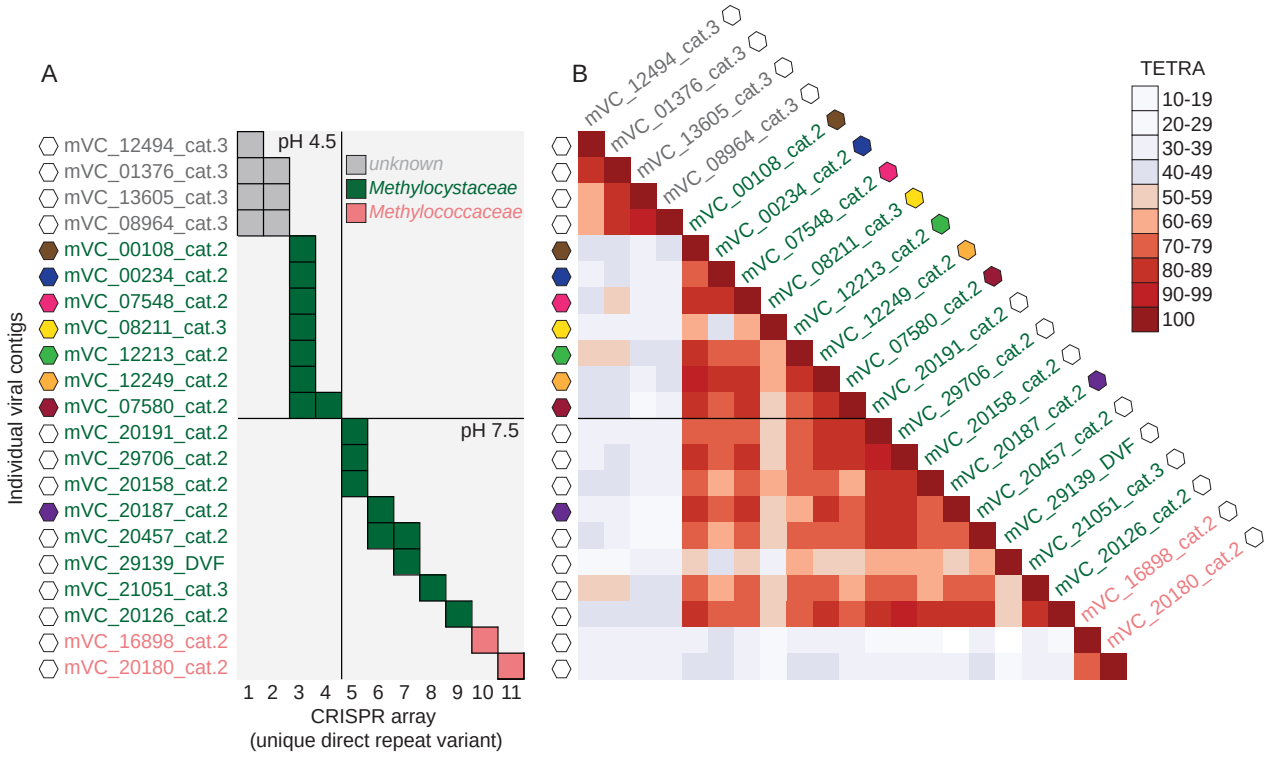
A
B
pH 4.5
pH 7.5
unknown
Methylocystaceae
Methylococcaceae
Individual viral contigs
CRISPR array
(unique direct repeat variant)
1 2 3 4 5 6 7 8 9 10 11
mVC_12494_cat.3
mVC_01376_cat.3
mVC_13605_cat.3
mVC_08964_cat.3
mVC_00108_cat.2
mVC_00234_cat.2
mVC_07548_cat.2
mVC_08211_cat.3
mVC_12213_cat.2
mVC_12249_cat.2
mVC_07580_cat.2
mVC_20191_cat.2
mVC_29706_cat.2
mVC_20158_cat.2
mVC_20187_cat.2
mVC_20457_cat.2
mVC_29139_DVF
mVC_21051_cat.3
mVC_20126_cat.2
mVC_16898_cat.2
mVC_20180_cat.2
TETRA
10-19
20-29
30-39
40-49
50-59
60-69
70-79
80-89
90-99
100

A

Order	Family	Cat 1	Cat 2	Cat 3
Rhizobiales	*Methylocystaceae*	1	38	41
	Hyphomicrobiaceae		1	3
	Various Rhizobia families	1	4	
Methylococcales	*Methylococcaceae*		4	6
Myxococcales	Various families			3
Bdellovibrionales	*Bdellovibrionaceae*		1	

Methanotroph viruses
Non-methanotrophic methylotroph viruses
Predator viruses

B

Methylocystaceae viruses (80)

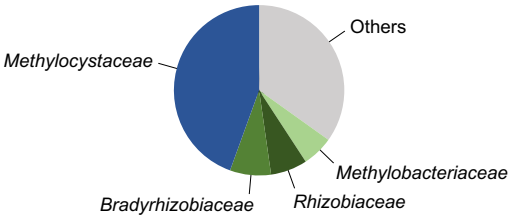

Methylococcaceae viruses (10)

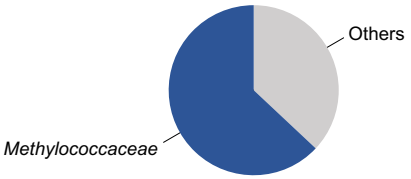

Hyphomicrobiaceae viruses (4)

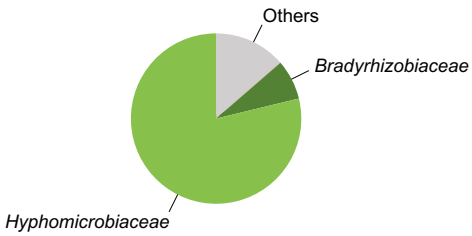

Bdellovibrionaceae virus (1)

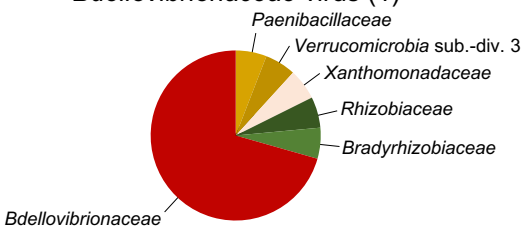

Rhizobia viruses (5)

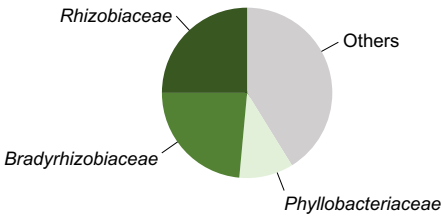

Myxococcales viruses (3)